MODELING OF SELECTED PHENOMENA GOVERNING SURFACE ICING

Janusz Sznajder

Institute of Aviation
Department of Aerodynamics and Flight Mechanics
Krakowska Av. 110/114, 02-256 Warsaw, Poland
tel.: +48 22 8460011 ext 492, fax: +48 22 8464432
e-mail: jsznaj@ilot.edu.pl

Abstract

Atmospheric icing poses a threat for safety in many areas of transport, especially in air transport and exerts harmful impact on operation of external sensors and mechanisms of aircraft, ships and land vehicles. In order to investigate phenomena leading to ice accretion on sensitive parts of objects exposed to icing conditions numerical simulation models are in use. These models are typically composed of submodels dealing with a fragment of the complex phenomenon of ice accretion and its interaction with external flow. A practical approach to simulation of icing process is to divide it into three problems being solved interactively: 1) simulation of two-phase flow of air and dispersed supercooled water and determination of distribution of mass of water hitting the object's surface, 2) determination of conditions on the surface collecting supercooled water from the external flow and simulation of freezing and water film flow, and 3) modification of computational grid as a consequence of change of shape of the surface with deposits of ice. A simulation system directed at investigation of atmospheric icing on moving object is being developed as an extension of capabilities of a commercial CFD code ANSYS FLUENT. Solutions of two-phase flow of air and dispersed water with specific boundary conditions enabling the determination of distribution of water hitting the surface, as well as results of modelling of water film flow on the surface will be presented. The system of equations describing the transport of the dispersed water consists of the continuity and momentum equations. It is assumed, that interactions between the phases are onedirectional, i.e. the air flow influences the water droplet flow and not vice-versa. It is also assumed that the water film velocity distribution is linear in direction normal to surface. This way, both phenomena are being described with first order partial differential equations with respect to space and time and the solution approaches may be similar.

Keywords: icing, transport, air transport, simulation, two-phase flow

Introduction

The aim of this paper is to present the details of the approach to determine the distribution of water captured by a body in an external two-phase flow consisting of air and dispersed water droplets (water collection efficiency) and the approach to model the surface water film flow. The typical composition of numerical tools engaged in the simulation of atmospheric icing and the flow of information is shown in Fig. 1, based on methodology applied in [1]. The splitting of the problem of simulation of ice accretion and its interaction with the flow into separate problems is a practical solution resulting from the necessity of simultaneous application of two different two-phase flow models (one model for external air-dispersed droplets flow and second model for water film flow on the surface) as well as the necessity of applying sequential cycles of flow computations and grid modifications. Two approaches are generally applied in numerical computations of water collection efficiency of a surface. Chronologically the first of them is Lagrangian approach [6, 7], tracking the motion of a droplet in space. With current stage of development of codes of Computational Fluid Dynamics more insight into the flow field of dispersed water may be gained from Eulerian approach solving the two-phase flow in the entire computational domain as in [1, 3]. The model of droplet-phase presented here flow was built following the Eulerian approach, with assumption of oneway coupling between the phases (droplet flow is affected by air flow and itself does not affect it), which is used for low water concentration, typical for problems of atmospheric icing [0].

Modular approach for the simulation of icing effects:

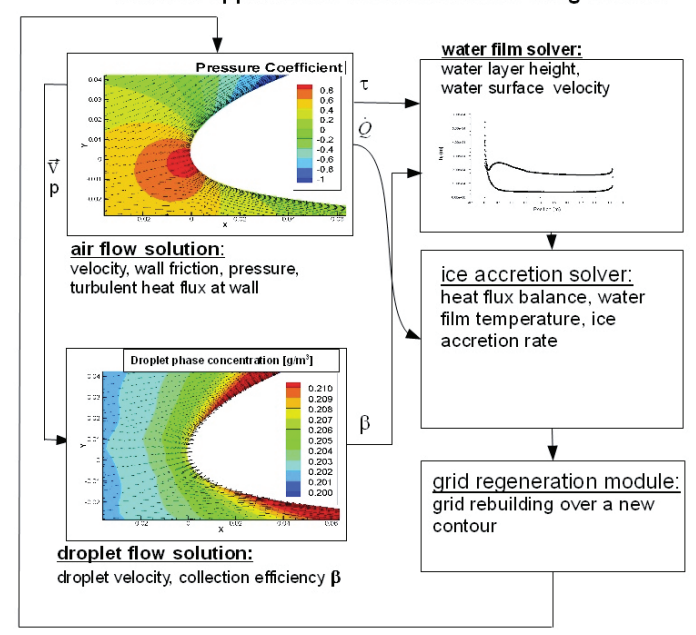


Fig. 1. Partitioning of the method of simulation of icing effects into sub-problems analysed with different numerical tools

A model of water surface film flow was built using data – water collection efficiency – computed by the dispersed phase flow model. Its results – distribution of water film height and velocity may be used as input for water freezing and ice accretion solver, currently under development.

This paper addresses the issue of implementation of the dispersed-water flow and water surface-film flow models using as an example a two-dimensional airfoil. Also effects of some important flow parameters such as droplet size, dispersed-phase density, airfoil angle of attack on the distribution of collected water are addressed.

1. Flow equations of the dispersed water phase

The model of air flow applied in the present approach consists of equations of conservation of mass, momentum and energy supplemented by turbulence equation (one-equation Spalart-Allmaras turbulence model). The system of equations is solved by the FLUENT solver in identical way as in the case of one-phase fluid flow. For the present work the pressure-based solver was selected with second order upwind discretization of flow variables and SIMPLE-type pressure-velocity coupling. The water-droplet-phase flow is described with the continuity equation:

$$\frac{\partial \rho_d}{\partial t} + \vec{\nabla} \cdot \rho_d \vec{U}_d = 0 \tag{1}$$

and the momentum conservation equation, written in the following, conservative form:

$$\frac{\partial \rho_d \vec{U}_d}{\partial t} + \vec{\nabla} \cdot (\rho_d \vec{U}_d) \vec{U}_d = \vec{f}_d + \rho_d \left(1 - \frac{\rho_a}{\rho_w} \right) \vec{g} - \frac{\rho_d}{\rho_w} \cdot \vec{\nabla} p , \qquad (2)$$

where:

 U_d – droplet velocity,

 ρ_d - droplet phase density, equal to $\alpha \cdot \rho_w$,

 α – droplet phase volume fraction,

 ρ_w – water density,

 ρ_a – air density,

 \vec{f}_d – drag force,

 \vec{g} – gravitational acceleration.

The FLUENT solver provides the possibility of computing the transport of a user-defined scalar ϕ_k solving the equation written in the following general form:

$$\frac{\partial \phi_k}{\partial t} + \nabla \cdot (\vec{\psi}\phi_k - \Gamma_k \cdot \phi_k) = S_{\phi k} , \qquad (3)$$

where $\vec{\psi}$ is a vector field and Γ_k diffusion coefficient of the scalar "k". In the present, two-dimensional case, three scalars were used to represent three variables: ρ_d , u_d , and v_d , where u_d and v_d are components of the droplet velocity \vec{U}_d . For each of them Equation (3) is solved in the computational domain. The components of the $\vec{\psi}$ vector are the products ρ_d u_d and ρ_d v_d . The scalar Γ in Equation (3) is set to zero. The computation of the advection terms in equation (1.1) and (2) is being accomplished in a user-defined procedure applying Gauss Divergence Theorem. The wall values of the $\vec{\psi}$ vector components are computed using an upwind scheme, based on cell centre values and gradients of scalars computed at the cell centres. The forces acting on the droplets taken into account include droplet drag, the net effect of gravity and buoyancy, and effect of pressure gradient in the flow field, as in [1, 3]. Drag force is computed using formula (4) proposed by Morrison [4] for a sphere, because of reported agreement with experimental data for a wide range of droplet Reynolds number from 0.01 up to 10^6 . Drag force per unit volume is evaluated by multiplying drag of a single droplet (sphere) by the factor ρ_d /($V_d \cdot \rho_w$), where V_d is droplet volume.

$$c_D = \frac{24}{\text{Re}} + \frac{2.6 \cdot \frac{\text{Re}}{5}}{1 + \left(\frac{\text{Re}}{5}\right)^{1.52}} + \frac{0.411 \left(\frac{\text{Re}}{263000}\right)^{-7.94}}{1 + \left(\frac{\text{Re}}{263000}\right)^{-8}} + \left(\frac{\text{Re}^{0.8}}{461000}\right). \tag{4}$$

Collection efficiency, β at a point of a surface is computed as:

$$\beta = \frac{\rho_d \, \vec{U}_d \cdot \vec{n}}{\rho_{d \, \text{inf}} \cdot \left| \vec{U}_{d \, \text{inf}} \right|},\tag{5}$$

where \vec{n} is a local surface normal vector, and $\rho_{d inf}$ is droplet phase density at large distance from airfoil. It is referred to also as Liquid Water Content (LWC) in the air.

Boundary conditions at domain external boundaries include pressure far-field on surfaces not affected by the body wake and pressure outlet on the rear surface affected by the wake. The air flow quantities being set on pressure far-field include Mach number, X and Y components of the vector of the flow direction, pressure and temperature. The water-droplet phase variables include mass concentration and X and Y components of the droplet velocity. It is assumed that the X and Y components of the air and water droplet velocity are equal in the far field. On the outlet surface only pressure and temperature are set. The air and water flow velocities and density include disturbances caused by the airfoil and are computed by the solver. On the airfoil surface the wall no-slip boundary condition is applied for the air flow. For the water flow there are two cases treated in different way. When water is intercepted by the surface, $(\vec{U}_d \cdot \vec{n}) < 0$, \vec{n} being the cell-wall normal vector, the airfoil surface is considered totally permeable for the water. The droplet-phase velocity on the surface is extrapolated using gradients computed in the cell centre. When $(\vec{U}_d \cdot \vec{n}) > 0$ the water concentration on the surface, ρ_d is set to zero, and the components of water flow velocity are extrapolated using gradients computed at the cell centre. This ensures continuity of droplet flow variables.

2. Results of computations of water collection efficiency

A comparison of the results of the present method with experimental results was done for NACA 23012 airfoil of chord equal 0.9144 m, at the angle of attack $\alpha = 2.5^{\circ}$. Free stream velocity was 78.23 m/s, far field pressure and temperature was 101,330 Pa and 299 K respectively. Liquid

Water Content (LWC) was set at 0.19 g/m^3 and medium droplet diameter was $20 \mu m$. The experimental results were reported in [5] and quoted in [3] and represented measured distribution of collection efficiency of a set of droplet sizes with Median Volumetric Diameter of $20 \mu m$. The computed characteristics of airfoil collection efficiency are shown in Fig. 2. The computations were performed on a mesh of 25,000 elements with the y+ parameter value ≥ 30 over most of the airfoil surface. The overall agreement between the experimental and computational results is good, especially the maximum value of β computed for normal distribution of droplet diameter is very close to the value obtained in experiment. The main differences between the computational and experimental results are the shift of the computed characteristics to the right (into the suction zone) and underprediction of β in the areas of low β which suggests overestimation of droplet drag. The difference of location of a maximum- β point is very small (1% of airfoil circumference).

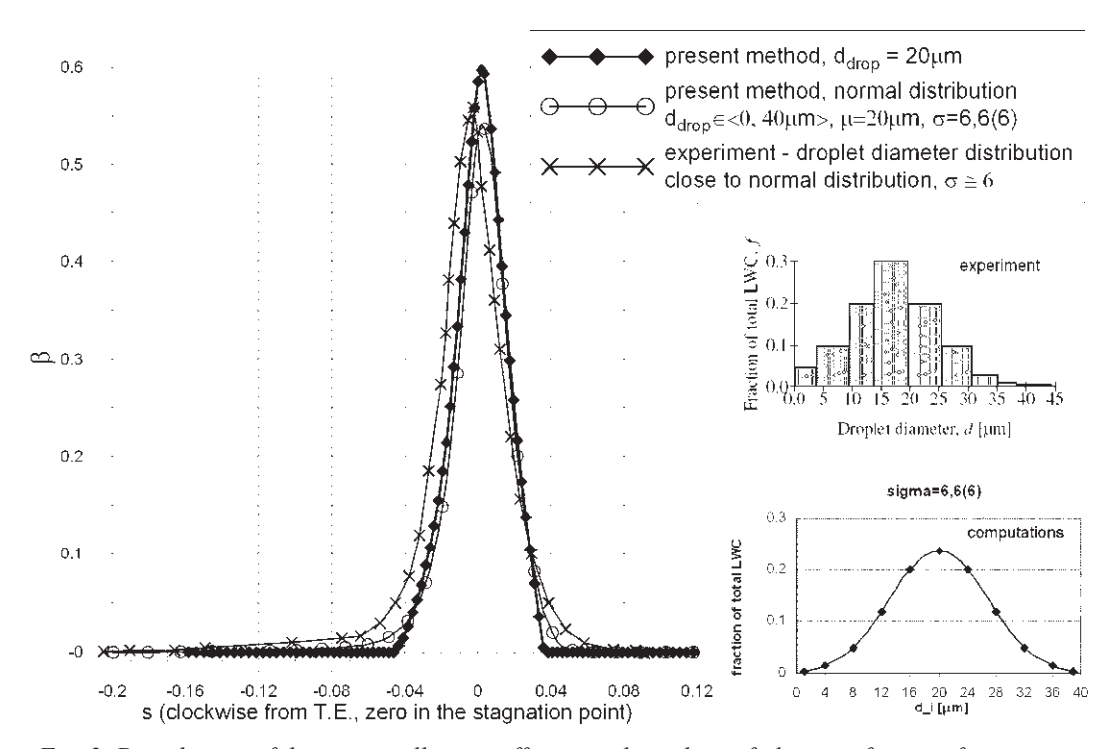


Fig. 2. Distribution of the water collection efficiency along the airfoil circumference, first test case

The airworthiness regulations, FAR25, appendix C [2] define icing conditions in terms of droplet median diameter against liquid water content for different temperature values (Fig. 4). It is therefore interesting to compare the results of mass flux of collected water computed for a single-diameter approximation of droplet distribution with results for different distributions of droplet size, since the computations for a single-droplet approximation of the droplet phase flow require much less time and resources than computations for a distribution of droplet size. A comparison of mass flux of collected water computed for single droplet distributions and conditions defined by t = -20°C and diameter of 20 µm in stratiform clouds (Fig. 4) with results obtained for three normal distributions of droplet size, each with medium diameter of 20 µm, diameter range of $\langle 0-40 \mu m \rangle$ and different values of standard deviation σ (Fig. 3) was done and the results are shown in Fig. 5. They indicate, that for the determination of mass of water collected by an airfoil, in conditions defined by the FAR 25 regulations (Fig. 4) a single-diameter droplet distribution model is justified.

3. Water film flow

If the temperature of supercooled droplets is sufficiently low, they may freeze on impact, producing so called rime icing. At higher temperatures, due to release of latent heat of freazing,

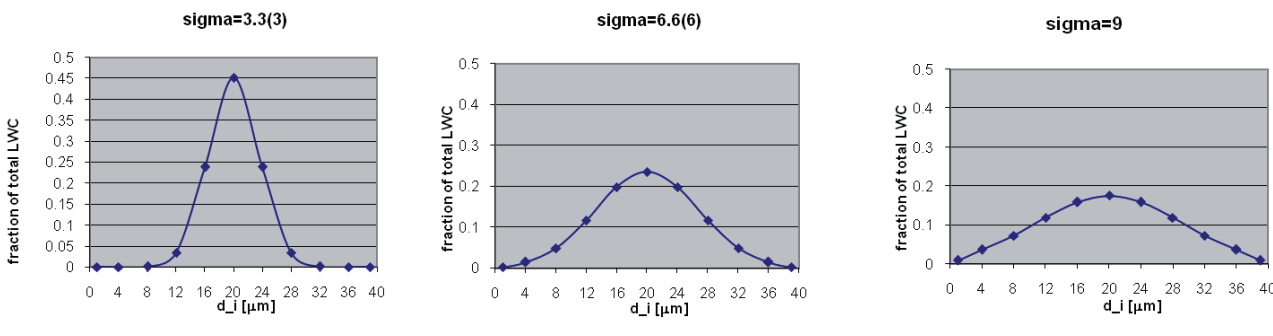


Fig. 3 Distributions of droplet diameter

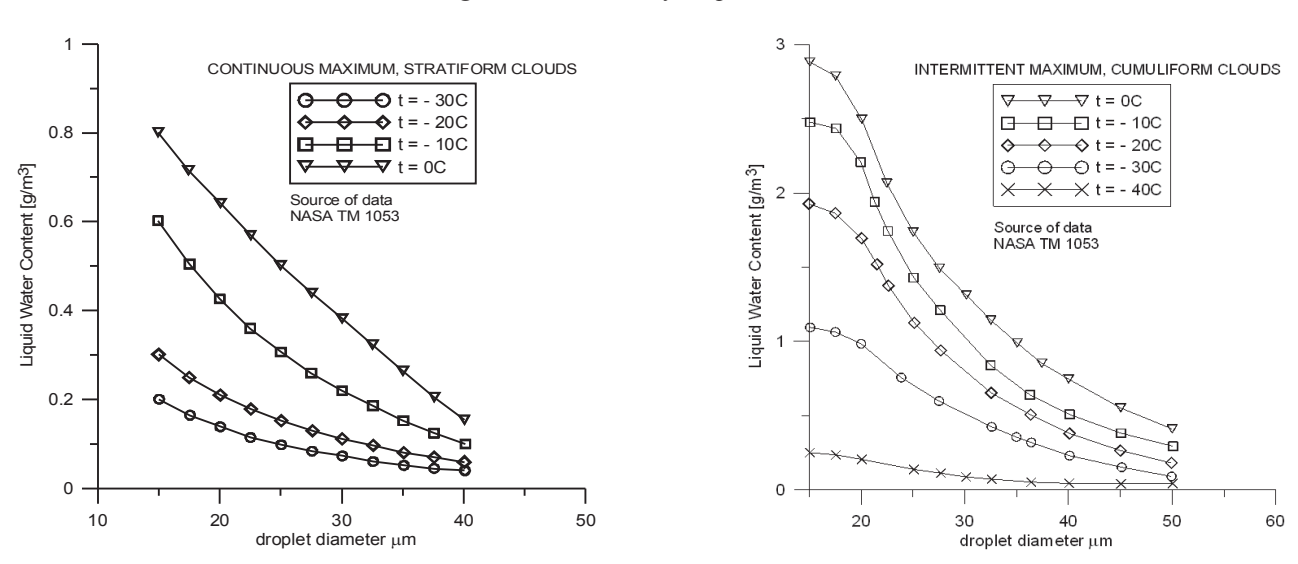


Fig. 4. Definition of continuous and intermittent icing conditions, FAR25 regulations, appendix C

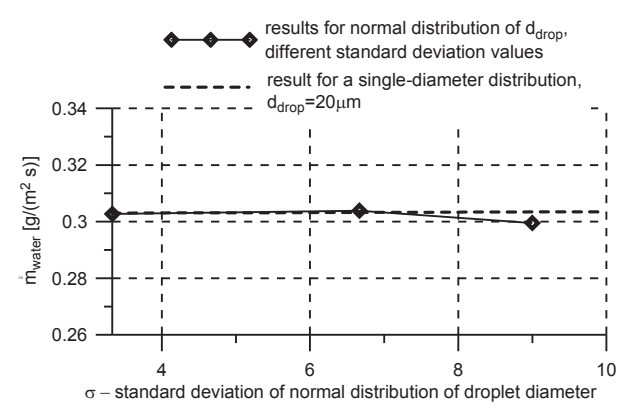


Fig. 5. Mass flux of water collected by airfoil at different values of σ . NACA 23012 airfoil at $\alpha = 2.5^{\circ}$, M = 0.22, Re = 4.5 mln, $LWC = 0.2g/m^3$

only a fraction of the incoming supercooled water freezes and the rest is transported along the surface as a thin water film driven along the surface mainly by shear stress resulting from the air flow. Its precise modelling requires a solution of two-phase flow problem of Volume of Fluid type. Due to complexity of such task on general, three-dimensional bodies, assumptions simplifying it are often in use. Morency et al. [0] assume linear distribution of velocity in water film in direction normal to surface. This way the movement of the water is described by the average film velocity and film height:

$$\overline{u}(x) = \frac{1}{h_f} \int_0^{h_f} u(x, y) dy , \qquad (6)$$

where h_f is the film height and y is the direction normal to surface.

Another assumption in [8] is, that due to low speed of water, compared to the air, the shear stress in air on the air-water interface is the same as in air passing solid wall. Because of continuity of shear stress in the air-water interface, the velocity in the film may be described as

$$u(x,y) = (y/\mu_w)\tau_{wall}(x).$$
 (7)

With these assumptions the equation for transport of water in the thin film is:

$$\rho_{w} \left[\frac{\partial h_{f}}{\partial t} + div(\vec{u}_{m}h_{f}) \right] = V_{\infty} \cdot LWC \cdot \beta - \dot{m}_{evap} - \dot{m}_{ice}, \qquad (8)$$

where \dot{m}_{evap} and \dot{m}_{ice} denote mass of water evaporating and freezing in unit time.

The structure of Equation (8) is the same as the structure of transport equation for a User-Defined Scalar in Fluent solver (3). The difficulty of using the Eq. 3 for the solution of transport of h_f is that the equation for scalar transport is solved in the entire computational domain, whereas the h_f is transported only on the surface. To solve this problem a user-defined function was created effectively separating the single-cell zone around the surface with water flow from the rest of the fluid. In this zone the Equation (8) was solved assuming no water evaporation and freezing. The results in terms of water film height and average x-velocity distributions are shown in Fig. 6 and Fig. 7.

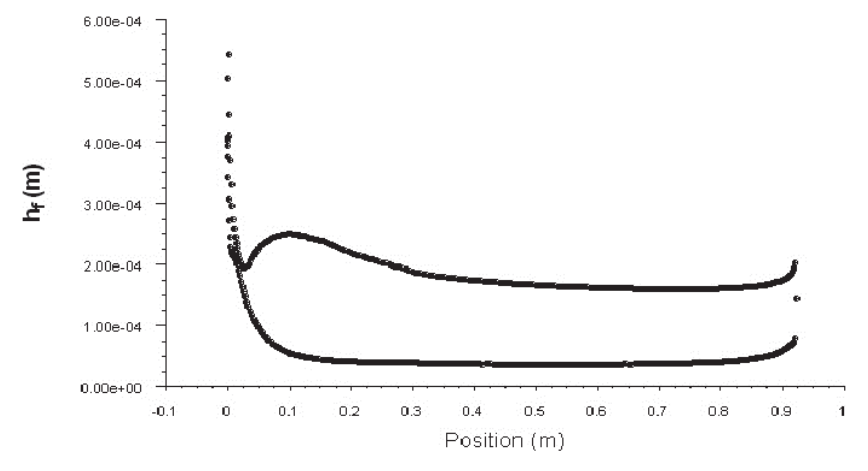


Fig. 6. Distribution of water film height on the surface of NACA 23012 airfoil in conditions of $\alpha=2.5$ °, M=0.22, Re=4.5 mln. LWC=0.2 g/m³, t=-20°C, $d_{drop}=20$ μm

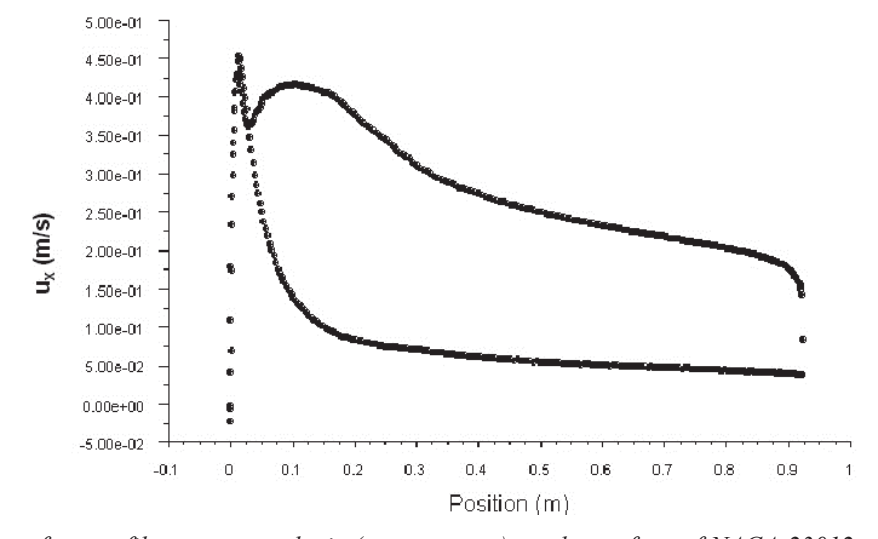


Fig. 7. Distribution of water film average velocity(x-component) on the surface of NACA 23012 airfoil in conditions of $\alpha = 2.5$ °, M = 0.22, Re = 4.5 mln. LWC = 0.2 g/m³, t = -20°C, $d_{drop} = 20$ μ m

4. Future work

The planned future work will be directed at extension of the surface water flow model to make it possible to determine the freezing fraction of water that accretes on a surface in unit time. It may be obtained from an energy balance equation:

$$\rho_{w} \left[\frac{\partial h_{f} C_{w} T}{\partial t} + div(\vec{v}_{m} h_{f} C_{w} T) \right] = \left[C_{w} T_{d,\infty} + \frac{\|u_{d}\|^{2}}{2} \right] \times V_{\infty} \cdot LWC \cdot \beta - 0.5 \left(L_{evap} + L_{subl} \right) \dot{m}_{evap} + \left(L_{fusion} - C_{ice} T \right) \dot{m}_{ice} + \sigma \left(T_{\infty}^{4} - T^{4} \right) + \dot{Q}_{h} + \dot{Q}_{cond}.$$

$$(9)$$

Equation (9) may be solved for T assuming that all water freezes on impact ($h_f = 0$). If T obtained this way is higher than $T_{freezing}$ then T is set to $T_{freezing}$ and set of Equations (6) and (9) may be solved for \dot{m}_{ice} .

5. Conclusions

A model of low-density droplet phase flow was developed and implemented in the FLUENT solver. The validation case represented flow conditions typical for small droplet, low Liquid Water Content, described by the FAR 25, Appendix C regulations – conditions of continuous icing in stratiform clouds. The water collection efficiency β characteristics computed with the present method are close to the characteristics obtained in experiment, with differences mainly in areas of low values of the β parameter. The present method slightly underestimates the collection efficiency for the conditions used for the test. The possible reason is overestimation of droplet drag. The computations for different shapes of normal distribution of droplet diameter distribution were aimed at exploring the possibility of using single droplet diameter for the determination of mass flux of collected water. Results of mass flux of collected water obtained for single diameter distribution and for normal distribution of droplet diameters with standard deviation of 1/6 of the assumed diameter range (a frequently applied model of normal distribution for random variations of parameters in technology) were practically identical. Computations for different values of angle of attack, within the range of its normal takeoff/landing, cruise values revealed that the lowest rate of water collection occurs at low profile drag values of angle of attack, without rapid growth at higher angles of attack. A two-parameter model describing water film flow on the surface, driven by shear stress resulting from air flow was also implemented using the system of User-Defined Scalars. Verification of assumptions made in formulating the model will be possible after the implementation of the model of determination of the distribution of freezing fraction of water.

References

- [1] Beaugendre, H., Morency, F., Habashi, W. G., FESNSAP-ICE's Three-Dimensional In-Flight Ice Accretion Module: ICE3D, Journal of Aircraft, Vol. 40, No. 2, 2003.
- [2] Federal Aviation Regulations FAR 25 Appendix C, hhttp://www.flightsimaviation.com/data/FARS/part_25-appC.html.
- [3] Hospers, J. M., Hoeijmakers, H. W. M., *Eulerian Method for Ice Accretion on Multiple-Element Airfoils*, 7-th International Conference on Multiphase Flows, Tampa, FL, United States 2010.
- [4] Morrison, F. A., Data Correlation for Drag Coefficient for Sphere, www.chem.mtu.edu/~fmorriso/DataCorrelationForSphereDrag2010.pdf, Department of Chemical Engineering, Michigan Technological University, Houghton, MI, accessed October 2011.
- [5] Papadakis, M, Rachman, A, Wong, S.-C., Yeong, H.-W., Hung, K. E, Vu, G. T., Bidwell, C. S., Water Droplet Impingement on Simulated Glaze, Mixed and Rime Ice Accretions, Technical Report NASA/TM-2007-213961, NASA, 2007.

- [6] Potapczuk, M. G., Al-Khalil, K. M., Velazquez, M. T., *Ice Accretion and Performance Degradation Calculations with LEWICE/NS*, NASA Technical Memorandum 105972, AIAA-93-0173, Prepared for the 31st Aerospace Sciences Meeting and Exhibit, Reno, Nevada, United States 1993.
- [7] Szilder, K., Lozowski, E., *Numerical Simulation of Cloud Drop Inpingement on a Helicopter*, 27-th Congress of the Aeronautical Sciences, ICAS, 2010.
- [8] Morency, F., Tezok, F., Paraschivoiu, I., *Heat and Mass Transfer in the Case of Anti-Icing System Simulation*, Journal of Aircraft, Vol. 37. No. 2, 2000.